Mathematical model and finite-volume solution of a three-dimensional fluid flow between an eccentric cylinder and a cone

E. Kornaeva, L. Savin, A. Kornaev, V. Arkhipov

***Abstract*—**The goal of this paper is to detect and to justify the basic parameters and operational conditions in hydrodynamic seals with thin layer fluid flow when three–dimensionality of space, influence of inertia and viscous forces in consistent cannot be neglected. The mathematical model of three-dimensional enforced and shear fluid flow in an eccentric channel between a stationary outer cone and a rotating inner cylinder is based on the Navier-Stokes equation and the continuity equation. Such flows occur in the hydrodynamic seals and fluid–film bearings. On the basis of similarity theory and dimensional analysis the significance of the terms in the Navier–Stokes equation and the continuity equation were considered with the values of similarity criteria, such as Reynolds number, Euler number and others and geometry parameters, such as the eccentricity and conicity parameters. The numerical solution and simulation program are based on the finite-volume method with the calculation schemes, represented in this paper. The results represent velocity and pressure fields together with some integral characteristics e.g. leakage as a function of conicity and eccentricity. The results of numerical solutions were compared with results of widely known analytical solutions and with the results calculated by other numerical methods.

***Keywords*—**Cone-cylinder gap, finite volume, incompressible fluid, Navier-Stokes equation.

I. INTRODUCTION

MATHEMATICAL modeling of enforced and shear flows of viscous fluids in gaps of various geometry is a topical question in hydrodynamics. Among examples of such flows are flows in noncontact hydrodynamic seals and fluid-film bearings which are widely used in mechanical engineering, metallurgical and rocket industry. It is widely known that there are many life-time and reliability requirements for seals and bearings [1], [2].

Mathematical and simulation models of the three–dimensional enforced and shear flow of viscous incompressible fluid in the gap between the steady state cone and the rotating eccentric cylinder are studied in this article. The main equations in this mathematical model are the Navier-Stokes equation and the continuity equation [3]. The three-dimensional flow in the channel under study, the thickness of which is variable in all directions, does not allow to use traditional approaches to form a problem of the thin layers of fluid flow in the fluid-film bearings and the hydrodynamic seals. For example, as it will be shown below, it is impossible to omit inertia terms and some dissipative terms of the Navier-Stokes, i.e. it is impossible to use the Reynolds equation [3] or variation approach described in [4], [17]. In this case, the present research focuses on the numerical solution of the Navier-Stokes equation system considering all the inertia and dissipative terms.

This work was supported in part by the Ministry of Education and Science of the Russian Federation under the projects No. 9.101.2014/K and No. 363 of a part of the state task for the "State University - ESPC" in 2015, and under grant of the President of the Russian Federation No 14.Z56.14.6000-MK.

E. P. Kornaeva is with the Education-Science-research institute of information technologies, State University – Education-Science-Production Complex, Oryol, 302020, Russia (corresponding author to provide phone: +7953-817-30-50; e-mail: lenoks_box@mail.ru).

L. A. Savin is with the Faculty of New Technologies and Production Automation, State University – Education-Science-Production Complex, Oryol, 302020, Russia (e-mail: savin@ostu.ru).

A. V. Kornaev is with the Faculty of New Technologies and Production Automation, State University – Education-Science-Production Complex, Oryol, 302020, Russia (e-mail: rusakor@inbox.ru).

V. P. Arkhipov is with the Faculty of New Technologies and Production Automation, State University – Education-Science-Production Complex, Oryol, 302020, Russia (e-mail: varhipov@inbox.ru)

II. MODELING

A. Mathematical model

The flow of the viscous incompressible Newtonian fluid in the confusor is under investigation. The flow region is formed by the stationary truncated cone (stator) and the rotating cylinder (rotor), which are shown in Fig. 1. The Cone has radii R_1 and R_2 respectively. The Cylinder with radius r is off-centered in cone and is rotating at a constant angular velocity ω. Under pressure P_1 the fluid flows from one end towards the channel shrinkage and escapes from the other end under pressure P_0.

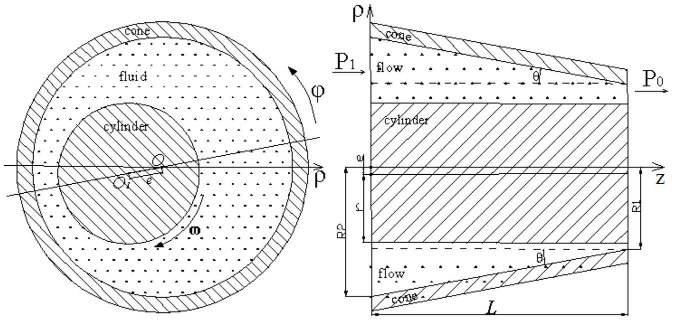

Fig. 1 geometry of the channel

The fluid is assumed to fill up the whole channel, the flow is laminar. The temperature is assumed as constant.

The Navier-Stokes equation and the continuity equation are the fundamental equations which describe the flow process [3], [5] and in tensor form look like:

$$\begin{cases} \rho_0 \nabla \cdot \left(\vec{V} \otimes \vec{V} \right) = -\nabla P + \nabla \cdot D_\sigma, \\ \nabla \cdot \vec{V} = 0, \end{cases} \tag{1}$$

where ρ_0 is a density of fluid, $\vec{V}$ is a velocity vector, ∇P is a gradient of the pressure, D_σ is a stress deviator, $\nabla \cdot \vec{V}$ is a velocity divergence, $\otimes$ is a tensor product.

The stress deviator is determined by the Newton's generalized hypothesis:

$$D_\sigma = 2\mu D_\xi, \tag{2}$$

where μ is a coefficient of the dynamic viscosity, D_ξ is a strain-rate deviator.

For the incompressible medium:

$$T_\xi = D_\xi = \frac{1}{2}\left(\nabla \otimes \vec{V} + \vec{V} \otimes \nabla \right). \tag{3}$$

Due to the nondimensionalization by means of characteristic quantities, system (1) in cylindrical coordinates can be rearranged as follows:

$$\begin{cases} \delta^2 \hat{V}_\rho \dfrac{\partial \hat{V}_\rho}{\partial \hat{\rho}} + \delta \dfrac{\hat{V}_\varphi}{\hat{\rho}+\psi} \dfrac{\partial \hat{V}_\rho}{\partial \varphi} + \delta^2 \hat{V}_z \dfrac{\partial \hat{V}_\rho}{\partial \hat{z}} - \dfrac{\hat{V}_\varphi^2}{\hat{\rho}+\psi} = -Eu \dfrac{\partial \hat{P}}{\partial \hat{\rho}} + \\ + \dfrac{\delta}{Re}\left(\dfrac{\partial^2 \hat{V}_\rho}{\partial \hat{\rho}^2} + \dfrac{1}{\hat{\rho}+\psi} \dfrac{\partial \hat{V}_\rho}{\partial \hat{\rho}} + \dfrac{1}{(\hat{\rho}+\psi)^2} \dfrac{\partial^2 \hat{V}_\rho}{\partial \varphi^2} + \delta^2 \dfrac{\partial^2 \hat{V}_\rho}{\partial \hat{z}^2} - \right. \\ \left. - \dfrac{\hat{V}_\rho}{(\hat{\rho}+\psi)^2} - \dfrac{2}{\delta (\hat{\rho}+\psi)^2} \dfrac{\partial \hat{V}_\varphi}{\partial \varphi} \right), \\ \delta \hat{V}_\rho \dfrac{\partial \hat{V}_\varphi}{\partial \hat{\rho}} + \dfrac{\hat{V}_\varphi}{\hat{\rho}+\psi} \dfrac{\partial \hat{V}_\varphi}{\partial \varphi} + \delta \hat{V}_z \dfrac{\partial \hat{V}_\varphi}{\partial \hat{z}} + \delta \dfrac{\hat{V}_\rho \hat{V}_\varphi}{\hat{\rho}+\psi} = \\ = -Eu \dfrac{1}{\hat{\rho}+\psi} \dfrac{\partial \hat{P}}{\partial \varphi} + \dfrac{1}{Re}\left(\dfrac{\partial^2 \hat{V}_\varphi}{\partial \hat{\rho}^2} + \dfrac{1}{\hat{\rho}+\psi} \dfrac{\partial \hat{V}_\varphi}{\partial \hat{\rho}} + \right. \\ \left. + \dfrac{1}{(\hat{\rho}+\psi)^2} \dfrac{\partial^2 \hat{V}_\varphi}{\partial \varphi^2} + \delta^2 \dfrac{\partial^2 \hat{V}_\varphi}{\partial \hat{z}^2} - \dfrac{\hat{V}_\varphi}{(\hat{\rho}+\psi)^2} + \dfrac{2\delta}{(\hat{\rho}+\psi)^2} \dfrac{\partial \hat{V}_\rho}{\partial \varphi} \right), \\ \delta \hat{V}_\rho \dfrac{\partial \hat{V}_z}{\partial \hat{\rho}} + \dfrac{\hat{V}_\varphi}{\hat{\rho}+\psi} \dfrac{\partial \hat{V}_z}{\partial \varphi} + \delta \hat{V}_z \dfrac{\partial \hat{V}_z}{\partial \hat{z}} = -\delta Eu \dfrac{\partial \hat{P}}{\partial \hat{z}} + \\ + \dfrac{1}{Re}\left(\dfrac{\partial^2 \hat{V}_z}{\partial \hat{\rho}^2} + \dfrac{1}{\hat{\rho}+\psi} \dfrac{\partial \hat{V}_z}{\partial \hat{\rho}} + \dfrac{1}{(\hat{\rho}+\psi)^2} \dfrac{\partial^2 \hat{V}_z}{\partial \varphi^2} + \delta^2 \dfrac{\partial^2 \hat{V}_z}{\partial \hat{z}^2} \right), \\ \dfrac{\partial \hat{V}_\rho}{\partial \hat{\rho}} + \dfrac{\hat{V}_\rho}{\hat{\rho}+\psi} + \dfrac{1}{\delta} \dfrac{1}{\hat{\rho}+\psi} \dfrac{\partial \hat{V}_\varphi}{\partial \varphi} + \dfrac{\partial \hat{V}_z}{\partial \hat{z}} = 0, \end{cases} \tag{4}$$

where $\hat{\rho} = \dfrac{\rho - (r-e)}{h_{02}+e}$, $\hat{z} = \dfrac{z}{L}$ are non-dimensional radial and axes coordinates, $\hat{V}_\rho = \dfrac{V_\rho}{\delta V^*}$, $\hat{V}_\varphi = \dfrac{V_\varphi}{V^*}$, $\hat{V}_z = \dfrac{V_z}{V^*}$ are non-dimensional radial, tangential and axes components of the velocity vector $\hat{\vec{V}}$, $\hat{P} = \dfrac{P-P_0}{\Delta P}$ is a non-dimensional pressure function, $\delta = (\xi+1)(\beta+\eta\gamma)$, $\psi = \left(\gamma - \xi(\beta+\eta\gamma)\right)\delta^{-1}$, $\beta = \dfrac{R_2-R_1}{L}$, $\gamma = \dfrac{r}{L}$, $\eta = \dfrac{h_{01}}{r}$, $\xi = \dfrac{e}{h_{02}}$ are non-dimensional coefficients and geometric parameters, $Re = \dfrac{\rho_0 V^* \left(h_{02}+e\right)}{\mu}$, $Eu = \dfrac{\Delta P}{\rho_0 (V^*)^2}$ are Reynolds and Euler numbers respectively, V^* is a characteristic velocity, $h_{0j} = R_j - r$ is a radial clearance, e is a eccentricity.

The equations of the channel boundaries may be shown as follows:

$$\hat{R}(\hat{z}) = -\beta\delta^{-1}\hat{z} + 1,$$

$$\hat{r}(\varphi) = \delta^{-1}(\xi(\beta+\eta\gamma)(1+\cos(\varphi-\alpha)) - \gamma + \\ + \sqrt{1-\xi^2(\beta+\eta\gamma)^2 \sin^2(\varphi-\alpha)}), \quad \varphi \in [0;2\pi].$$

System (4) can be solved with boundary conditions simultaneously. The boundary conditions for the velocity components can be presented as follows:

$$\begin{cases} \hat{V}_\rho(\hat{r}(\varphi),\varphi,\hat{z}) = 0, \\ \hat{V}_\varphi(\hat{r}(\varphi),\varphi,\hat{z}) = \dfrac{\omega r}{V^*}, \\ \hat{V}_z(\hat{r}(\varphi),\varphi,\hat{z}) = 0, \end{cases} \quad \begin{cases} \hat{V}_\rho(\hat{R}(\hat{z}),\varphi,\hat{z}) = 0, \\ \hat{V}_\varphi(\hat{R}(\hat{z}),\varphi,\hat{z}) = 0, \\ \hat{V}_z(\hat{R}(\hat{z}),\varphi,\hat{z}) = 0. \end{cases} \tag{5}$$

For pressure function $\hat{P}$ on the ends of canal:

$$\hat{P}(\hat{\rho},\varphi,0) = 1, \ \hat{P}(\hat{\rho},\varphi,1) = 0. \tag{6}$$

Because the fluid flow canal is closed form the tangential coordinate direction the periodical conditions can be described as follows:

$$\hat{F}_i(\hat{\rho},0,\hat{z}) = \hat{F}_i(\hat{\rho},2\pi,\hat{z}), \ \frac{\partial \hat{F}_i(\hat{\rho},0,\hat{z})}{\partial\varphi} = \frac{\partial \hat{F}_i(\hat{\rho},2\pi,\hat{z})}{\partial\varphi}. \tag{7}$$

B. Analyses of model

As was said before, the flows in noncontact seals and fluid-film bearings are investigated, so the flow thickness is very small. The set of main parameters and theirs order of magnitudes are presented in Table I.

I The main parameters order of magnitudes

Parameter	Lower level	Upper level
r, m	10^{-2}	10^{-1}
h_{01}, m	10^{-5}	10^{-4}
β	0	10^{-1}
L, m	10^{-2}	10^{-1}
n, rpm	10^{1}	10^{5}
ΔP, Pa	10^{5}	10^{7}
μ, Pa·s	10^{-5}	10^{0}
ρ_0, kg/m^3	10^{0}	10^{3}

Using order-of-magnitude analysis it is easy to determining which terms in the equations are very small relative to the other terms [1], [3], [6], [7]. The values of the terms of equations (4) are presented in Table II, the geometry parameter δ coefficient domain is 10^{-4} to 10^{-1}. In order to δ coefficient two cases available, firstly, if the conicity parameter β has the same magnitude with the relative gap η, and secondly, if the conicity parameter β exceeds the relative gap η by one or more orders of magnitude. Also the Euler number Eu and the Reynolds number Re orders of magnitude are considered in follow conclusions:

- if the conicity parameter β is less than 10^{-3} and the Reynolds number is less than 10^{0}, then the velocity radial component, the inertial term and the velocity components derivatives in the tangential and axes directions are negligible;
- if the Reynolds number is more than 10^{0}, then the inertial terms and the viscosity terms has the same magnitude, and if the conicity parameter β is more or equal to 10^{-3}, all the velocity components has significant values.

II Equation (4) terms order of magnitudes

The Navier-Stokes equation										
Inertial terms $\hat{\nabla}\cdot\left(\hat{\vec{V}}\otimes\hat{\vec{V}}\right)$				$\hat{\nabla}\hat{P}$	Dissipative terms $\hat{\nabla}\cdot\hat{D}_\sigma$					
δ^2	δ^2	δ^2	δ	Eu	$\frac{\delta}{Re}$	$\frac{\delta^2}{Re}$	$\frac{\delta^3}{Re}$	$\frac{\delta^3}{Re}$	$\frac{\delta^3}{Re}$	$\frac{\delta^2}{Re}$
1	1	1	δ	Eu	$\frac{1}{\delta Re}$	$\frac{1}{Re}$	$\frac{\delta}{Re}$	$\frac{\delta}{Re}$	$\frac{\delta}{Re}$	$\frac{1}{Re}$
1	1	1	-	Eu	$\frac{1}{\delta Re}$	$\frac{1}{Re}$	$\frac{\delta}{Re}$	-	-	$\frac{\delta}{Re}$
The continuity equation										
1			δ			1		1		

According to the order-of-magnitude analysis, widely used assumptions of hydrodynamic theory of lubrication [3], [6] are acceptable if the conicity parameter β is less than 10^{-3}, and that is the flow between two cylinders actually. In this study it is necessary to consider the Navier-Stokes equation in its complete form.

Thus, the mathematical model of the researched process has a look (4)-(7) and consists of four nonlinear partial differential equations with four unknown functions.

III. NUMERICAL CALCULATIONS

Numerical calculations of equations (4)-(7) are based on the finite (or control) volume method (F.V.M.). By means of the F.V.M. it is possible to get an adequate solution even for a crude mesh, because of guaranteed fulfilling of the fundamental laws of conservation [8], [9].

Equations (4) in tensor form look as follows:

$$\begin{cases} \hat{\nabla}\cdot\left(\hat{\vec{V}}\otimes\hat{\vec{V}}\right) = -Eu\hat{\nabla}\hat{P} + \dfrac{1}{Re}\hat{\nabla}\cdot\left(\hat{\nabla}\otimes\hat{\vec{V}} + \hat{\vec{V}}\otimes\hat{\nabla}\right), \\ \hat{\nabla}\cdot\hat{\vec{V}} = 0, \end{cases} \tag{8}$$

where $\hat{\nabla}$ – a non-dimensional Hamiltonian operator.

According to the flow region geometry the element size by $O\rho$ direction is variable and depends on the $O\varphi$ coordinate. The element sizes measured with the $O\varphi$ and Oz coordinates are constant. See Fig. 2 as the discretization principle visualization in case of the coaxial flow region.

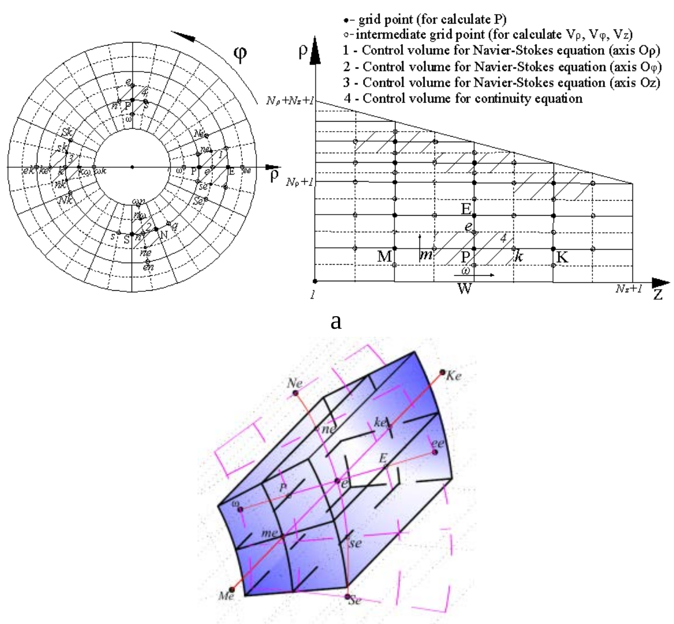

a

b

Fig. 2 Flow region discretization: (a) -radial and axial section and (b) – 3-d FV for Navier-Stokes equations (axis $O\rho$)

According to approach [8] - [15] the following operation is the volume integration of equations (8) in each finite volume: $d\hat\Omega = \hat\rho d\hat\rho d\varphi d\hat z$, shown in the Fig. 2 in a curvilinear coordinate system.

Using the Ostrogradskii formula it is possible to decrease the digit of the derivatives of the velocity vector:

$$\begin{cases} \int\limits_{\hat S_i} \hat n_i \cdot \left(\hat{\vec V} \otimes \hat{\vec V}\right) d\hat S_i = -Eu \int\limits_{\hat\Omega} \hat\nabla \hat P d\Omega + \\ + \dfrac{1}{Re} \int\limits_{\hat S_i} \vec n_i \cdot \left(\hat\nabla \otimes \hat{\vec V} + \hat{\vec V} \otimes \hat\nabla\right) d\hat S_i, \\ \int\limits_{\hat S_i} \vec n_i \cdot \hat{\vec V} d\hat S_i = 0. \end{cases} \tag{9}$$

where $\vec n_i$ is a unit normal vector on the respectively surface of FV.

When we calculate surface integrals on each FV surface (Fig. 2) and use the mean-value theorem, velocity components in the Navier-Stokes equations can be approximated by the exponential functions, e.g. $\hat V_\rho$ component of the first equation in each FV $[\hat\rho_e;\hat\rho_{ee}]$ looks as follows:

$$\hat V_\rho = \hat V_{\rho e} + \left(\hat V_{\rho ee} - \hat V_{\rho e}\right) \frac{\exp(\delta \hat V_\rho Re(\hat\rho - \hat\rho_e)) - 1}{\exp(\delta \hat V_\rho Re\Delta\hat\rho) - 1}.$$

After that system (9) turns to:

$$\begin{cases} -\hat a_e \hat V_{\rho_e} + \hat a_E \hat V_{\rho_{ee}} + \hat a_P \hat V_{\rho_\omega} + \hat a_{ne} \hat V_{\rho_{Ne}} + \hat a_{se} \hat V_{\rho_{Se}} + \\ + \hat a_{ke} \hat V_{\rho_{Ke}} + \hat a_{me} \hat V_{\rho_{Me}} = Eu\Delta\varphi\Delta\hat z(\hat\rho_e + \psi)\hat P\Big|_P^E + \\ + \dfrac{\Delta\hat\rho\Delta\hat z}{Re} \dfrac{\hat V_\varphi}{\hat\rho + \psi}\Bigg|_{se}^{ne}, \\ -\hat a_n \hat V_{\varphi_n} + \hat a_{ne} \hat V_{\varphi_{en}} + \hat a_{n\omega} \hat V_{\varphi_{\omega n}} + \hat a_N \hat V_{\varphi_q} + \hat a_P \hat V_{\varphi_S} + \\ + \hat a_{nk} \hat V_{\varphi_{kn}} + \hat a_{nm} \hat V_{\varphi_{mn}} = Eu\Delta\hat\rho\Delta\hat z \hat P\Big|_P^N + \dfrac{\delta\Delta\hat\rho\Delta\hat z}{Re} \dfrac{\hat V_\rho}{\hat\rho + \psi}\Bigg|_P^N, \\ -\hat a_k \hat V_{z_k} + \hat a_{ke} \hat V_{z_{ek}} + \hat a_{k\omega} \hat V_{z_{\omega k}} + \hat a_{nk} \hat V_{z_{Nk}} + \hat a_{sk} \hat V_{z_{Sk}} + \\ + \hat a_K \hat V_{z_{kk}} + \hat a_P \hat V_{z_m} = \delta Eu\Delta\varphi \dfrac{(\hat\rho + \psi)^2}{2}\Bigg|_{k\omega}^{ke} \hat P\Big|_P^K, \\ \hat b_e \hat V_{\rho_e} - \hat b_\omega \hat V_{\rho_\omega} + \hat b_n \hat V_{\rho_n} - \hat b_s \hat V_{\rho_s} + \hat b_k \hat V_{\rho_k} - \hat b_m \hat V_{\rho_m} = 0, \end{cases} \tag{10}$$

where $\hat a_E = \dfrac{\delta^2(\hat\rho_E + \psi)\hat F_E}{\exp(\delta Pe_E) - 1}$,

$$\hat a_{ne} = \frac{\delta \hat F_{ne}}{\exp((\hat\rho_{ne} + \psi)Pe_{ne}) - 1},$$

$$\hat a_P = \delta^2(\hat\rho_P + \psi)\hat F_P\left(1 + (\exp(\delta Pe_P) - 1)^{-1}\right),$$

$$\hat a_{se} = \delta \hat F_{se}\left(1 + \left(\exp\left((\hat\rho_{se} + \psi)Pe_{se}\right) - 1\right)^{-1}\right),$$

$$\hat a_{ke} = \frac{\delta^2 \hat F_{ke}}{2\Delta\hat\rho}\left((\hat\rho_{ke} + \psi)^2 - (\hat\rho_{me} + \psi)^2\right)\left(\exp\left(\frac{Pe_E}{\delta}\right) - 1\right)^{-1},$$

$$\hat a_{me} = \frac{\delta^2 \hat F_{me}\left((\hat\rho_{ke} + \psi)^2 - (\hat\rho_{me} + \psi)^2\right)}{2\Delta\hat\rho}\left(1 + \left(\exp\left(\frac{Pe_{me}}{\delta}\right) - 1\right)^{-1}\right),$$

$$\hat a_e = \hat a_E + \hat a_P + \hat a_{ne} + \hat a_{se} + \hat a_{ke} + \hat a_{me},$$

$$\hat F_{E(P)} = \hat V_{\rho_{E(P)}} \Delta\varphi\Delta\hat z,\ \hat F_{ne(se)} = \hat V_{\varphi_{ne(se)}} \Delta\hat\rho\Delta\hat z,$$

$$\hat F_{ke(me)} = \hat V_{z_{ke(me)}} \Delta\hat\rho\Delta\varphi,\ Pe_{E(P)} = Re\hat V_{\rho_{E(P)}} \Delta\hat\rho,$$

$$Pe_{ne(se)} = Re\hat V_{\varphi_{ne(se)}} \Delta\varphi,\ Pe_{ke(me)} = Re\hat V_{z_{ke(me)}} \Delta\hat z \text{ etc.}$$

System (10) is a discrete analogue of (8), and some of its coefficients include unknown functions discrete solution.

Due to the Navier-Stokes equation consisting non-linear terms, the solution search procedure is iterative. Using the first three equations of the system (10), with an approximate pressure distribution $\hat P^S$ an approximate velocity distribution $\hat{\vec V}^S$ is calculated, i.e. the equation system is solved of the following form:

$$A_V \hat{\vec V}^S = f(\hat P^S, \hat{\vec V}_\Omega),$$

where $A_V = (\hat{a}_{ij})$ are coefficients before increments of velocity components in the Navier-Stokes equation in all nodes of discrete flow region, $\hat{P}^S$ - approximate pressure distribution, $\hat{\hat{V}}_\Omega$ - the values of the velocity components on the border of the area.

The solution of this equation system is implemented using the Gauss–Seidel method, the convergence is provided by the sufficient attribute [8]:

$$\hat{a}_{ii} \geq \sum_{i \neq j} \hat{a}_{ij} \text{ - for all equation}$$

$$\text{and } \hat{a}_{ii} > \sum_{i \neq j} \hat{a}_{ij} \text{ - at least one equation}$$

The fulfillment of this condition is provided by the feature of the matrix A_V coefficients, for which the diagonal elements equal the sum of side elements with all the corresponding unknown components of velocity, for instance, for the first equation: $\hat{a}_{ii} = \sum_{i \neq j} \hat{a}_{ij}$.

The fulfillment of the second condition is provided by the known components of velocity on the boundary of the area, i.e. by the boundary conditions setting, so the corresponding side components move to the right-hand part, thus decreasing the sum of the remaining $\sum_{i \neq j} \hat{a}_{ij}$.

Next, the system (10) can be written for each unknown function, presented in a form of a sum of its value on the previous iteration and some increment $\hat{h}_F^{S+1}$: $\hat{F}^{S+1} = \hat{F}^S + \hat{h}_F^{S+1}$.

The results of the zero iteration can be taken as the solution of some asymptotic problem.

Then the equation system for the increments $\hat{h}_F^{S+1}$ calculation on every iteration can be obtained by means of subtraction of the corresponding equations on the previous step S from the first three equations of the system (10) on the $S+1$ step, adding the continuity equation to close the system on the $S+1$ step:

$$\begin{cases}
-\hat{a}_e \hat{h}_{\rho_e}^{S+1} + \hat{a}_E \hat{h}_{\rho_{ee}}^{S+1} + \hat{a}_P \hat{h}_{\rho_\omega}^{S+1} + \hat{a}_{ne} \hat{h}_{\rho_{Ne}}^{S+1} + \hat{a}_{se} \hat{h}_{\rho_{Se}}^{S+1} + \\
+ \hat{a}_{ke} \hat{h}_{\rho_{Ke}}^{S+1} + \hat{a}_{me} \hat{h}_{\rho_{Me}}^{S+1} - \hat{b}_E \hat{h}_{P_E}^{S+1} + \hat{b}_E \hat{h}_{P_P}^{S+1} = 0, \\
-\hat{a}_n \hat{h}_{\varphi_n}^{S+1} + \hat{a}_{ne} \hat{h}_{\rho_{en}}^{S+1} + \hat{a}_{n\omega} \hat{h}_{\varphi_{\omega n}}^{S+1} + \hat{a}_N \hat{h}_{\varphi_q}^{S+1} + \hat{a}_P \hat{h}_{\varphi_s}^{S+1} + \\
+ \hat{a}_{nk} \hat{h}_{\varphi_{kn}}^{S+1} + \hat{a}_{nm} \hat{h}_{\varphi_{mn}}^{S+1} - \hat{b}_N \hat{h}_{P_N}^{S+1} + \hat{b}_N \hat{h}_{P_P}^{S+1} = 0, \\
-\hat{a}_k \hat{h}_{z_k}^{S+1} + \hat{a}_{ke} \hat{h}_{z_{ek}}^{S+1} + \hat{a}_{k\omega} \hat{h}_{z_{\omega k}}^{S+1} + \hat{a}_{nk} \hat{h}_{z_{Nk}}^{S+1} + \hat{a}_{sk} \hat{h}_{z_{Sk}}^{S+1} + \\
+ \hat{a}_K \hat{h}_{z_{kk}}^{S+1} + \hat{a}_P \hat{h}_{z_m}^{S+1} - \hat{b}_K \hat{h}_{P_K}^{S+1} + \hat{b}_K \hat{h}_{P_P}^{S+1} = 0, \\
\hat{c}_e \hat{h}_{\rho_e}^{S+1} - \hat{c}_\omega \hat{h}_{\rho_\omega}^{S+1} + \hat{c}_n \hat{h}_{\varphi_n}^{S+1} - \hat{c}_s \hat{h}_{\varphi_s}^{S+1} + \hat{c}_k \hat{h}_{z_k}^{S+1} - \hat{c}_m \hat{h}_{z_m}^{S+1} = \\
= -\hat{c}_e \hat{V}_{\rho_e}^S + \hat{c}_\omega \hat{V}_{\rho_\omega}^S - \hat{c}_n \hat{V}_{\varphi_n}^S + \hat{c}_s \hat{V}_{\varphi_s}^S - \hat{c}_k \hat{V}_{z_k}^S + \hat{c}_m \hat{V}_{z_m}^S,
\end{cases}$$

where $\hat{b}_E = Eu\Delta\varphi\Delta\hat{z}(\hat{\rho}_e + \psi)$, $\hat{b}_N = Eu\Delta\hat{\rho}\Delta\hat{z}$,

$\hat{b}_K = 0.5\delta Eu\Delta\varphi((\hat{\rho}_{ke} + \psi)^2 - (\hat{\rho}_{k\omega} + \psi)^2)$,

$\hat{c}_{e(\omega)} = \left(\hat{\rho}_{e(\omega)} + \psi\right)\Delta\varphi\Delta\hat{z}$, $\hat{c}_{n(s)} = \delta^{-1}\Delta\hat{\rho}\Delta\hat{z}$,

$\hat{c}_{k(m)} = 0.5\Delta\hat{\rho}\Delta\varphi\left(\left(\hat{\rho}_e + \psi\right)^2 - \left(\hat{\rho}_\omega + \psi\right)^2\right)$.

It is more convenient to write this system down in a matrix form:

$$\begin{pmatrix} A_V & B_P \\ C_V & 0 \end{pmatrix} \begin{pmatrix} \hat{\hat{h}}_V^{S+1} \\ \hat{h}_P^{S+1} \end{pmatrix} = \begin{pmatrix} 0 \\ f(\hat{\hat{V}}^S) \end{pmatrix}, \tag{11}$$

where B_P are coefficients before increments of pressure in the Navier-Stokes equation, C_V are coefficients before increments of velocity components in the continuity equation, $f(\hat{\hat{V}}^S)$ is a right-hand part of the discrete analogue of the continuity equation, which includes the values of the velocity components on the previous iteration.

Matrix (11) includes zeroes block because of the continuity equation, so this matrix determinant approaches zero and its inversion is difficult to reach. As the result, the system of these equations may be solved as follows: express in terms of the vector of velocity increments in the first equation of (11) and set it in the second equation (11). Hereby we can, in the first place, find pressure increments and then - velocity components increment.

The coefficients of the system of equations discrete analogue include exponential functions of the velocity components approximation (Fig.3). Further, those exponential functions can be approximated by means of the power functions as polynomials of fifth order [8]. Here the coefficients which are first on the list are shown as follows:

$$\hat{a}_E = \begin{cases}
-\delta Pe_E f_E, & APe_E < -10 \\
-\delta Pe_E f_E + (1 + 0.1\delta Pe_E)^5 f_E, & \delta Pe_E \in [-10;0] \\
(1 - 0.1\delta Pe_E)^5 f_E, & \delta Pe_E \in (0;10] \\
0, & \delta Pe_E > 10
\end{cases}$$

$$\hat{a}_P = \begin{cases}
0, & \delta Pe_P < -10 \\
(1 + 0.1\delta Pe_P)^5 f_P, & \delta Pe_P \in [-10;0] \\
\delta Pe_P f_P + (1 - 0.1\delta Pe_P)^5 f_P, & \delta Pe_P \in (0;10] \\
\delta Pe_P f_P, & \delta Pe_P > 10
\end{cases}$$

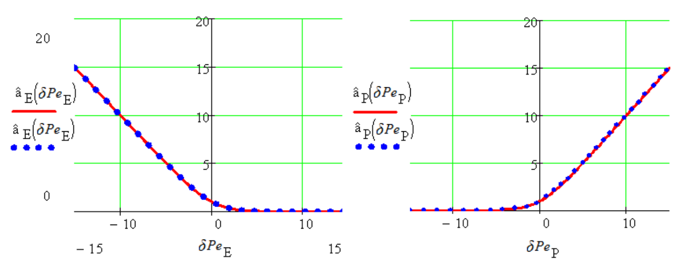

Fig. 3 the coefficient approximation

The approximation accuracy in the range under factors study is less than 0.1%, and such substitution significantly decreases the calculation time.

IV. DISCUSSION

Below some simulated results for the viscous incompressible fluid enforced and shear flow in the eccentric gap between the outer cone and the inner cylinder with input data are presented (see Table III).

III The input data definition

Pressure drop ΔP, Pa	Frequency n, rpm	Radius r, m
3.5×10^5	400	0.1
Gap h_{01}, m	Length L, m	Eccentricity e, m
2×10^{-4}	0.1	0.2 h_{01}
Conicity β	Density ρ_0, kg/m^3	Viscosity μ, Pa·s
1.0×10^{-3}	894.5	0.62

The velocity distributions axial component with respect to length and thickness, both in the region of the maximal gap is presented in Fig. 4. As it can be seen in Fig. 4 the maximum velocity value is reached on the lip of the channel.

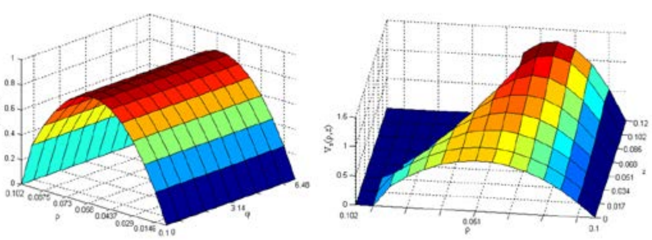

Fig. 4 axial velocity component: (a) - over a normal and tangential coordinate at the inlet and (b) - over a normal and axial coordinate

Under constrains of the axial pressure difference and the inner cylinder rotation, pressure in the axial direction is nonlinear with extremum point as shown in Fig. 5a. Also, in Fig. 5b the pressure appearance in the tangential direction with the maximum point in the thinnest gap region, which defines the bearing capacity of the lubricant layer.

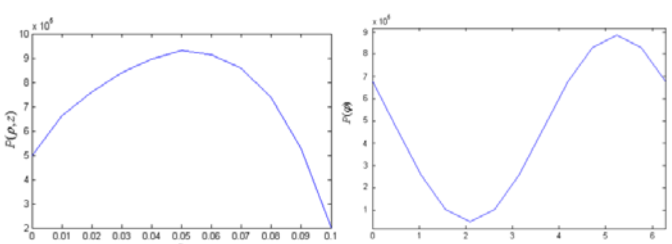

Fig.5 Pressure function: (a) - in the axial and (b) - tangential direction

Considering the simulation results it is established that the eccentricity increase leads to the nonlinear leakage increase. The conicity parameters increase with a fixed gap at the inlet of the channel leads to the drop in leakage (Fig.6).

Also, for the case of the enforced flow in the small nonzero conicity and the zero eccentricity region simulation the results were compared with the approximate solution of G. Nikitin [16], [17]. The result of this comparison is about 1% error in 1 degree region conicity, however, the error increases as the apex angle of the cone increases.

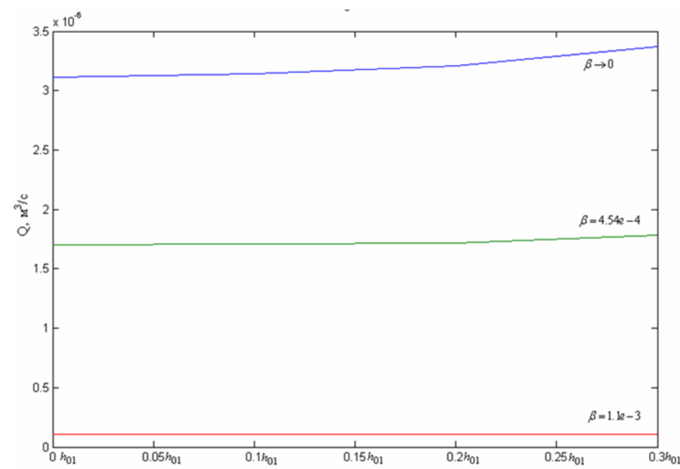

Fig. 6 Leakage as a function of conicity and eccentricity

For the case of coaxial and zero conicity flow region the results were compared with a well-known analytical solution and with other results simulated by the finite element method (FEM) and the finite difference method (FDM). The results of such comparison of various methods simulation are presented in table IV.

IV The simulation error

Number of layers through thickness	25	50	75
Max. error (FDM), %	11.3	5.44	3.56
Max. error (FEM), %	3.67	2.42	1.51
Max. error (FVM), %	2×10^{-3}	8.3×10^{-4}	2.5×10^{-4}

Obviously, the FV method has smallest percentage of error and adequate results even on a crude mesh.

V. CONCLUSION

So, the paper presents the mathematical model of a viscous incompressible fluid flow in a channel between a stationary cone and an eccentric rotating cylinder. This model is different from the known models of the fluid flow in the fluid-film bearings [3], [6], [18]-[20] in the following ways: firstly, it allows to consider a simultaneous action of the pressure and the shear flow, secondly, it takes a variable channel geometry into account, and it finally allows to consider the influence of the inertia forces on the basic physical values fields. The mathematical model was initially transformed into a non-dimensional form, which allowed to implement an analysis of the influence of every term of the equations. It was determined that for the flows in a cylinder-cone channels, where the conisity parameter is not higher than $\beta < 10^{-3}$ the Reynolds assumptions [3] are valid regarding the smallness of the normal velocity component and the velocities derivatives over the tangential and axial coordinates, and regarding the insignificant change in pressure over a layers thickness. For the cases, when conisity $\beta \geq 10^{-3}$ and the number $\mathrm{Re} > 10^{0}$ it is necessary to consider the inertia terms and the influence of the normal velocity component; it is also important to consider the change in pressure over the layers thickness and the channels length. As a result, the solutions based on the presented mathematical model, in light of its complexity, were obtained numerically. The discrete analogue of the model was obtained based in the method of finite volumes, effectiveness of which is caused by implementation of the conservation laws in every elementary volume, which makes it different from all other mesh methods. Using specific examples it was shown that calculation schemes based on the FVM allow to obtain adequate results even on a crude mesh.

Acknowledgment

The authors would like to thank to organizing committee of the 19th International Conference on Circuits, Systems, Communications and Computers, (CSCC 2015) for the possibility for us to publish this article in the NAUN journal.

References

[1] A.V. Ivanov, V.A. Korobchenko and A.V. Shostak, *Design of the seals of pumps wet end and turbo–pump assemblies in liquid rocket engine*, Voronezh State University, 2005 (in Russian).
[2] W. Todd Lindsey and Dara W. Childs, “The effect of convergine and divergin axial taper on the rotordynamic coefficients of liquid annular pressure seals”. *Theory versus experiment, ASME*,2000, pp. 126–131.
[3] H. Yukio, *Hydrodynamic Lubrication*. Tokyo: Springer, 2006, 250p.
[4] L. Savin, A. Kornaev and E. Kornaeva, “Variational principle in the hydrodynamic lubrication theory”. *International Journal of Mathematical Models and Methods in Applied Sciences*, vol. 9, 2015, pp. 114-119.
[5] G. A. Korn and T. M. Korn, *Mathematical Handbook for Scientists and Engineers.* Dover Publications, 2000.
[6] L.M. Milne-Thomson, *Theoretical hydrodynamics*. Fours edition, London: Macmilan and Co LTD, 1960.
[7] M.G. Khanovich, *Film–lubrication bearings*. Moskow, 1963 (in Russian).
[8] S. V. Patankar, *Numerical Heat Transfer and Fluid Flow*. McGraw-Hill, Hemisphere Publishing Corporation, 1980.
[9] J. Li and Z. Chen, “A new stabilized control volume method for the stationary Stokes equations”. *Adv. Comput. Math.* vol. 30, 2009, pp. 141–152.
[10] S.H. Chou, “Analysis and convergence of a covolume method for the generalized Stokes problem”. *Math. Comput*. vol. 66, 1997, pp.85–104.
[11] S.R. Sabbagh-Yazdi, M.T. Alkhamis, M. Esmaili and N.E. Mastorakis, “Finite volume analysis of two-dimensional strain in a thick pipe with internal fluid pressure”. *International Journal of Mathematical Models and Methods in Applied Sciences*, vol. 2, 2008, pp.162-167.
[12] A. Z. Szeri and A. Al-Sharif, “Flow Between Finite, Steady Rotating Eccentric Cylinders”. *Theoretical and Computational Fluid Dynamics*, vol. 7, 1995, pp. 1–28.
[13] C. Shu, L. Wang, Y. T. Chew and N. Zhao, “Numerical study of eccentric Couette-Taylor flows and effect of eccentricity on flow patterns”. *Theoretical and Computational Fluid Dynamics*, vol. 18, 2004, pp. 43–59.
[14] S. S. Bahrainian, “Adjustment of Dissipative Terms to Improve Two and Three- Dimensional Euler Flow Solutions”. *WSEAS Transactions on Fluid Mechanics*, vol. 5, 2010, pp. 1-14.
[15] H. Abbassi, S. Turki and S.B. Nasrallah, “Interpolation functions in control volume finite element method”, *Computational Mechanics*, vol.30, 2003, pp.303-309.
[16] V.A. Martsinkovskiy, *Rotor vibration of centrifugal machine: Hydrodynamics of restrictor canals*, Ukraine: SumDU, 2002.
[17] G.A. Nikitin, *“Groove and labyrinth seals of hydraulic aggregates”*, Moskow: Mashinostroenie, 1982, (in Russian).
[18] L. Savin, A. Kornaev and E. Kornaeva, “Theoretical aspects of modeling fluid film flow in journal bearings and seals”. *XIIth International Scientific-Technical conference “Seals and sealing technology of machines and devices”*. Worclaw – Kudowa Zdroj, Poland, 2010, pp. 39-42.
[19] Cai-Wan Chang-Jian and Chao-Kuang Chen, “Nonlinear dynamic analysis of a flexible rotor supported by micropolar fluid film journal bearings”. *International journal of engineering Science*, vol. 44, 2006, pp. 1050-1070.
[20] L. Savin, E. Kornaeva and A. Kornaev, “Modeling of fluid flow in the gap of cone-cylinder seals”. *XIIth International Scientific-Technical conference “Seals and sealing technology of machines and devices”*. Worclaw – Kudowa Zdroj, Poland, 2010, pp. 34-38.